CHARACTERIZING SPECTRAL FEATURES OF WATER-ICE, LUNAR REGOLITH SIMULANTS, AND THEIR MIXTURES AT THE VIS-NIR REGION. N. de Castro[1] and S. Li[1], [1] University of Hawai'i at Mānoa, Honolulu HI 96822, ninacwdc@hawaii.edu.

Introduction: On August 4th, 2022 the Korea Aerospace Research Institute (KARI) and NASA launched ShadowCam, a high-resolution camera specifically designed to map lunar Permanently Shadowed Regions (PSRs) and water-ice deposits [1]. This camera uses a spectral filter of 460-900 nm, centered at 700 nm at a 1.7 m/pixel resolution, offering, for the first-time, high-quality single band images of the lunar PSRs [1]. However, diagnostic reflectance features of water-ice under varying particle sizes, viewing geometries, and ice abundances are still poorly constrained, posing important limitations for interpreting the upcoming ShadowCam data.

Our study aims to characterize diagnostic spectral features of water-ice, lunar regolith simulants, and their mixtures at the visible (VIS) to near infrared (NIR) region (350-2,500 nm). We investigated variations in reflectance with varying 1) particle sizes of water-ice, 2) viewing geometry, and 3) water-ice content. Overall, characterizing diagnostic spectral features of water-ice in the laboratory is fundamental for interpreting the potentially large spectral variations in VIS-NIR data acquired by ShadowCam and any future missions interested in the remote sensing of water-ice.

Experiment Setups:

Pure Water-Ice. We nebulized water droplets in liquid nitrogen inside a freezer to form ice particles and sieved them into particle size groups of 20-32 μm, 32-45 μm, 45-53 μm, 53-63 μm, 63-75 μm, 75-90 μm, 90-106 μm, and 106-125 μm, and 125-180 μm.

An ASD FieldSpec 4 spectrometer was fixed onto a goniometer to control the phase angle (*g*) in each experiment. The goniometer acted as a principal plane and we set the light source and the sensor to the desired incidence (*i*) and emittance (*e*) angles for each experiment. For the particle size experiments with pure water-ice, the phase angle was fixed at 30° (*i*= 30°, *e*= 0°). For the viewing geometry experiments with pure water-ice, the phase angle varied from -15° to 105° for each particle size group (*i* = 45°, *e* varied from +60° to -60° at 15° incrementations). The spectrometer was calibrated using a Labsphere Spectralon disk, as outlined in [2].

Water-ice and lunar simulant mixtures. We will use two lunar simulants to represent the Moon's main geological terrains in a laboratory environment: an anorthositic simulant representing the lunar highlands and a basaltic simulant to simulate mare rocks. We dehydrated the simulants by heating them for 5 days in a vacuum chamber at 350°C to remove terrestrial water in the simulants. We intimately mixed the ice and simulants in a freezer to simulate the intimate distribution of water-ice in the lunar regolith. The setup of the ASD spectrometer was the same as in the pure water-ice experiments.

The experiments with the water-ice and lunar simulant mixtures consisted of two parts. First, we varied the water-ice content in each particle size group at 1, 2, 5, 10, 15, 20, 25, 30, 40, and 50 wt.%, fixing the phase angle at 30°. Second, we studied the effects of viewing geometry on reflectance by varying the phase angle from -15° to 105° at 15° incrementations for each particle size group, at a low ice content scenario at ~2 wt.% and a high ice content scenario at ~15 wt.%.

Data Analysis: We analyzed the average reflectance of water-ice in the VIS region (0.65-0.75 μm), as well as the reflectance near 1.35, 1.85, and 2.25 μm that are out of ice absorptions. We also calculated the band depth of absorptions near 1.0, 1.2, 1.5, and 2.0 μm by performing a continuum removal analysis on the corrected spectra for the Spectralon artifacts.

Results:

Particle Size. Our results show that the averaged reflectance in the 450-950 nm region exhibits a steep decrease for particles less than ~100 μm and it varies little when the particle size is greater than ~100 μm (Fig. 1). The band depth of absorptions near 1.0, 1.2, 1.5, and 2.0 μm slightly increases in particle sizes smaller than ~50 - 60 μm, and they remain almost constants when the particle size varies from ~70 to > 200 μm (Fig. 2). While the correlation between particle size and band depths of the 1.5 and 2.0 μm absorptions is very weak (Fig. 2).

Viewing Geometry. The phase curves of pure water-ice show forward scattering for all particle size groups (Fig. 3). The curves are shaped by 1) a surge in average reflectance at ~zero phase and 2) the reflectance drops towards larger phase angles (~ 60°) and it increases from ~60° to 105° phase angle that is the highest phase angle in our experiments. The band depths of our examined absorptions near 1.0, 1.2, 1.5, and 2.0 μm are greatest at phase angles near 60°, regardless of the particle size group. (Fig. 4).

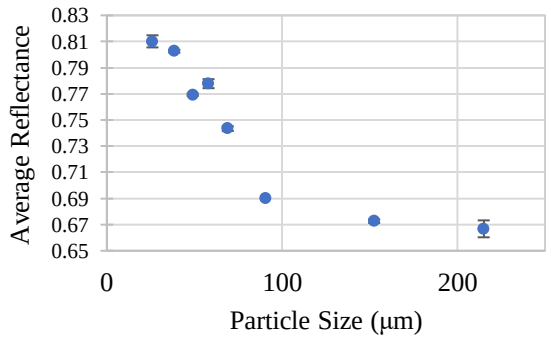

Figure 1. Variation in average reflectance with particle size in the VIS-NIR range (450-950 nm).

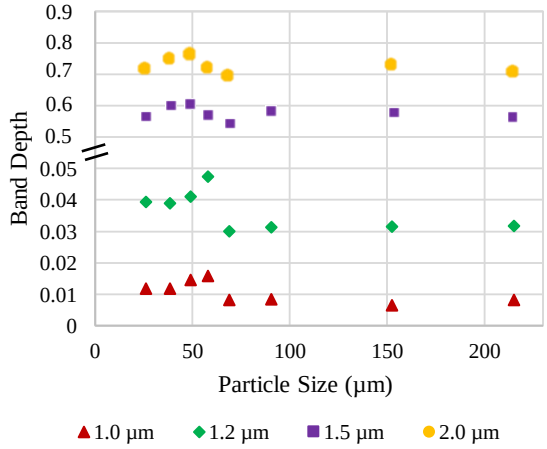

Figure 2. Band-depth as a function of particle size for the four characteristic absorption peaks of pure water-ice: 1.0 μm (A), 1.2 μm (B), 1.5 μm (C), and 2.0 μm (D).

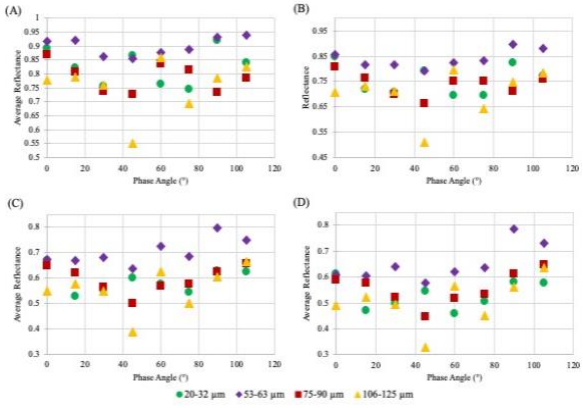

Figure 3. Phase curves of pure water-ice with varying particle sizes at the (A) 650-750 nm range, (B) 1350 nm, (C) 1850 ± 10 nm, and (D) 2250 ± 10 nm.

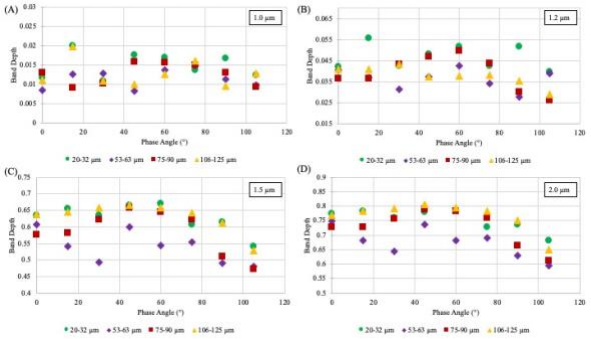

Figure 4. Band depth as a function of phase angle for four particle size groups of pure water-ice.

Discussion: The steep decrease in reflectance for water-ice particles less than 100 μm reflects a shift in scattering behavior (Fig. 1). In fine grain ice (<100 μm), multi-grain scattering dominates because photons are easily scattered into the neighboring grains due to short optical path lengths of fine ice particles [3]. In contrast, more photons are absorbed in coarser grains (> ~100 μm), which decreases the reflectance. The band depth of ice absorptions near 1.0 and 1.2 μm is sensitive to particle-size smaller than ~60 μm (Fig. 2). The strong absorptions near 1.5 and 2.0 μm exhibit very weak dependence on particle size and phase angles, which makes the two absorptions appropriate for estimating water-ice content.

We found that the optimal viewing geometry for water ice is independent of particle size. Based on our results in Fig. 3, we predict that the strongest reflectance for water-ice will be detected at high phase angles ≥105°. The optimal phase angles for observing the ice absorptions near 1.0, 1.2, 1.5, and 2.0 μm are near 60°.

Conclusion and future work: Our results show that the VNIR reflectance (350-2,500 nm) of water-ice exhibits strong dependance on particle size less than ~100 μm, and it remains almost constant at particle sizes greater than 100 μm. We recommend high phase angles (≥105°) for examining the VNIR reflectance of water ice and phase angles near 60° for observing ice absorptions near 1.0, 1.2, 1.5, and 2.0 um. We also note that the 1.5 and 2.0 μm absorptions are strong (> 50%) and show weak dependence on particle size and phase angle. These two absorptions are appropriate for estimating ice contents. Our ongoing work includes preparing intimate mixtures of water-ice and lunar simulants, performing spectral measurements of these mixtures, and analyzing their spectral features.

References: [1] Robinson M. et al. (2018) *Lunar Polar Volatiles Conference*, Abstract #5028. [2] Yang Y. et al. (2019) *Journal of Geophysical Research: Planets, 124*, 31-60. [3] Lucey P. G. and Clark R. N. (1985) *Ices in the Solar System*, 155-168.